Hierarchical Controlled Grid-Connected Microgrid based on a Novel Autonomous Current Sharing Controller

Guan, Yajuan; Quintero, Juan Carlos Vasquez; Guerrero, Josep M.

Published in:
Proceedings of the 2015 IEEE Energy Conversion Congress and Exposition (ECCE)

DOI (link to publication from Publisher):
10.1109/ECCE.2015.7309988

Publication date:
2015

Document Version
Early version, also known as pre-print

Hierarchical Controlled Grid-Connected Microgrid based on a Novel Autonomous Current Sharing Controller

Yajuan Guan, Juan C. Vasquez and Josep M. Guerrero
Research Programme on Microgrids www.microgrids.et.aau.dk
Department of Energy Technology Department
Aalborg University, Denmark
{ygu, juq, joz}@et.aau.dk

***Abstract*— In this paper, a hierarchical control system based on a novel autonomous current sharing controller for grid-connected microgrids (MGs) is presented. A three-level hierarchical control system is implemented to guarantee the power sharing performance among voltage controlled parallel inverters, while providing the required active and reactive power to the utility grid. A communication link is used to transmit the control signal from the tertiary and secondary control levels to the primary control. Simulation results from a MG based on two grid-connected parallel inverters are shown in order to verify the effectiveness of the proposed control system.**

Keywords*— Hierarchical control, autonomous current sharing controller, grid - connected microgrid.

I. INTRODUCTION

Distributed generation (DG) is emerging as a new paradigm to produce onsite highly reliable and good quality electrical power. These DG systems are powered by different kinds of renewable energy sources such as fuel cells, photovoltaics, wind energy, batteries, microturbines and so on. They can be connected to local low-voltage electric power networks, also called microgrid (MG) [1], [2], through power conditioning ac units, i.e., inverters or ac–ac converters, which can operate either in grid-connected mode or islanded modes [3] A MG involves different technologies, for example converters, advance control strategies, communications, and energy storage systems (ESSs).

Droop control method has been dominated the autonomous control of parallel inverters in the last decade in applications like parallel redundant uninterruptible power supply systems, distributed power systems, MGs, and so on [4], [6]. This well-known control technique consists of measuring active and reactive powers, adjusting locally proportionally frequency and amplitudes of each inverter output voltage in order to emulate the behavior of a synchronous generator. Although this technique only needs local information to operate, it presents a number of problems that were solved along the literature. Some control strategies were proposed to deal with these problems such as the derivative terms [6], [7], virtual impedance [8], [9] and reverse droop controller [10], [11]. However, the droop based control approaches have the inherent drawback which is the slow transient response due to the instantaneous active and reactive powers calculation and the limitation of the bandwidth of low pass filter [12].

Furthermore, the seamless transition between islanded and grid-connected modes is necessary for flexible MGs. In order to achieve these performances, hierarchical control based on droop control method is proposed to ac and dc MGs, providing functionalities defined in different control levels to mimic a large-scale power system [13]-[17]. The hierarchical control is able to achieve the power sharing performance among voltage controlled inverters (VCIs), while injecting the required dispatched power into the main grid.

In this paper, a hierarchical control system based on a novel autonomous current sharing controller for grid-connected parallel three-phase VCIs in MG is presented. In the primary control level, a novel autonomous current sharing controller which includes a synchronous-reference-frame (SRF) virtual impedance loop, a SRF phase-locked loop (SRF-PLL), and inner voltage and current loops have been employed to realize the current sharing among the parallel VCIs. The secondary control level is used to compensate the voltage magnitude and frequency deviations produced by the virtual impedance loop in the primary control. Besides, a frequency and magnitude synchronization loop is also included in secondary control to synchronize the output voltage of MG and the voltage of point of common coupling (PCC) before connecting to the main grid. The primary and secondary control levels can guarantee the power sharing performance and power supply quality in standalone operation, and then the tertiary control level is thereafter employed to perform the connection to the utility grid. By contrast, the control signal from secondary and tertiary control level will change the resonant frequency of the PR controller in primary control level to achieve the control performance. Simulation results from a two grid-connected paralleled VCIs system is shown to verify the effectiveness of the designed system.

The paper is organized as follows. Section II introduces the operation modes transition. Section III presents the configuration and design of the hierarchical control system. Simulation results are shown in Section IV. Section V concludes the paper.

978-1-4673-7151-3/15/$31.00 ©2015 IEEE

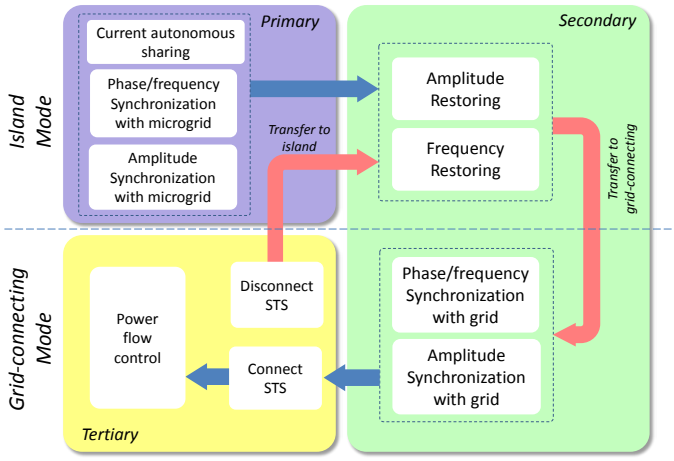

Fig.1. Functionality definition and operation modes transition

II. Operation Modes Transsition

The functionalities and modes transition of hierarchical controlled MG is shown in Fig.1. The primary control is a decentralized controller of a single VCI which is responsible for the direct and quadrature currents output sharing among the parallel VCIs.

As high power quality is usually required by local sensitive loads, secondary control is adopted for improving the power supply quality by restoring the voltage magnitude and frequency deviation to the nominal values in islanded mode. On other hand, in order to achieve the seamless transition from islanded mode to grid-connected mode, another voltage phase/frequency and amplitude synchronization loop is used for synchronizing the output voltage of one VCI to another, and for synchronizing the bus voltage of the MG with the voltage of grid utility before turning on the static switch (STS).

Tertiary control is activated to generate the voltage reference amplitude and phase increments according to active and reactive power commands from upper control level or power dispatch center. The amplitude and phase increments are sent back to the primary level to control VCIs to inject the dispatched power to the utility grid.

The MG can be seen as a load bus. The distribution lines between the MG and the PCC present high *R/X* ratio due to the short length and low voltage. Therefore, that the active and reactive powers (*P* and *Q*) are dominated by the voltage difference ($V_1 - V_2$) and the power angle (δ), respectively:

$$\delta \cong RQ/V_1V_2 \tag{1}$$

$$V_1 - V_2 \cong RP/V_1 \tag{2}$$

being V_1 and V_2 the voltages in the MG and the PCC, respectively.

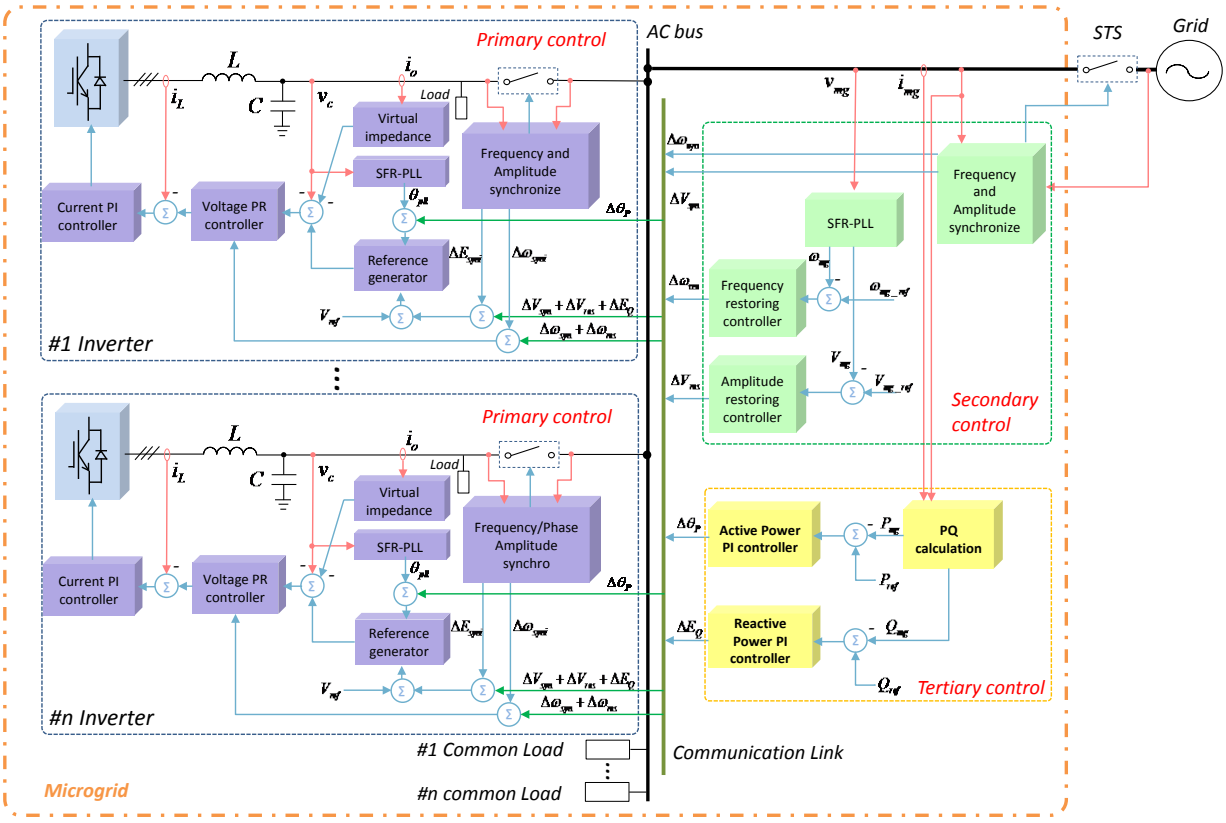

Fig.2. Control structure of the proposed hierarchical controlled microgrid

III. The Configuration and Design of the Hierarchical Control System

The three-level hierarchical control for the grid-connected MG based on a novel autonomous current sharing controller is organized as shown in Fig 2. The power stage of a VCI consists of a three-leg three-phase inverter connecting to a DC link, loaded by an L_f-C_f filter, and connected to the AC bus. The controller includes a SRF-PLL, a virtual resistance loop, a DC link voltage feed-forward loop, a proportional-resonant (PR) inner voltage loop (G_v) and a PI current loop (G_i) that generates a PWM signal to drive the IGBTs inverter gates. Inductor currents and capacitor voltages are transformed to the stationary reference frame ($i_{L\alpha\beta}$ and $v_{c\alpha\beta}$). Output currents are transformed to the synchronous reference frame (i_{odq}). All signals generated by secondary and tertiary control are transmitted to the primary control of VCI through communication links.

A. *Primary control level*

The primary control deals with the inner voltage and current control loops of each VCI and regulates the quadrature and direct current outputs by adding a SRF virtual impedance loop and a SRF-PLL as shown in Fig.3. The proposed controller supplies a voltage reference to the inner loops. The voltage reference V_{ref} is generated by using the amplitude reference ($|V_{ref}|$) and the phase generated by the SRF-PLL. Even though the PLL is trying to synchronize the inverter with the common AC bus, in case of supplying reactive loads, the quadrature current flowing through the virtual resistance will create an unavoidable quadrature voltage drop that will cause an increase of frequency in the PLL. In other words, the PLL will compel the inverter to be stable at a frequency point with zero phase delay (ZPD) obtained from the transfer function of the system. In this way, the mechanism inherently endows an $I_{oq}-\omega$ droop characteristic to each VCI. The transfer function of VCI is shown as follows:

$$T_{plant}(s)=\frac{G(s)\left[1+G_{Lequ}(s)Z_{line}(s)\right]}{1+G_{Lequ}(s)Z_{line}(s)+G_{vir}(s)G(s)+G_{Lequ}(s)Z_o(s)} \quad (3)$$

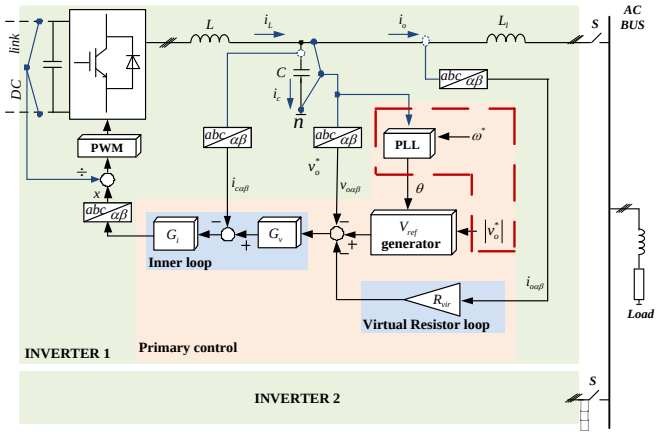

Fig. 3. Block diagram of the autonomous current-sharing control strategy.

where $G(s)$ represents the inner voltage and current control loop of inverter, $Z_o(s)$ is equivalent impedance of VCI, $G_{Lequ}(s)$ and $Z_{line}(s)$ are equivalent load network and line impedance, $G_{vir}(s)$ is virtual resistance loop. Therefore the relationship between i_{oq} *and* R_{vir} as well as ω can be derived from the following relationship

$$arc\tan\left[T_{plant}(j\omega)\right]=0^\circ \quad (4)$$

Similarly, in case of supplying active loads, the direct current flowing through the virtual resistance will drop the direct voltage, which will cause a decrease of amplitude in output voltage. So that an I_{od} -V droop characteristic is also supplied by the virtual resistance influence the amplitude of output voltage.

Considering the inherent mechanism of I_{od} with voltage amplitude and I_{oq} with frequency, a virtual resistance R_{vir} is employed to share the quadrature and direct load currents among the paralleled inverters.

Hence, the relationship of the common bus voltage, reference voltage, and output current vectors can be expressed in Euler form as follows:

$$\begin{aligned}\vec{V}_{bus}&=\vec{V}_{ref}-\vec{I}_o\cdot R_{vir}\\&=(V_{ref}\cos\varphi-I_o\cdot R_{vir}\cdot\cos\phi)+j(V_{ref}\sin\varphi-I_o\cdot R_{vir}\cdot\sin\phi)\end{aligned} \quad (5)$$

being φ the voltage reference angle and ϕ the output current angle.

Equation (5) can be also expressed in a synchronous reference frame by decomposing direct and quadrature components as follows

$$V_{bus}=V_{refd}-R_{vir}\cdot I_{od} \quad (6a)$$

$$0=V_{refq}-R_{vir}\cdot I_{oq} \quad (6b)$$

where V_{refd} and V_{refq} are the d axis and q axis component of each VCI's output-voltage references separately, and I_{od} and I_{oq} are d axis and q axis components of output current.

Thus, the relationship between I_{od} , I_{oq} and R_{vir} can be generalized and expressed for a number N of converters as

$$I_{od1}R_{vir1}=I_{od2}R_{vir2}=\ldots=I_{odN}R_{virN} \quad (7a)$$

$$I_{oq1}R_{vir1}=I_{oq2}R_{vir2}=\ldots=I_{oqN}R_{virN} \quad (7b)$$

Note that the d and q axis output currents of paralleled inverters are inversely proportional to their virtual resistances. In this way, the direct and quadrature currents sharing ratio of parallel VCIs can be directly adjusted by regulating the corresponding SRF virtual impedance of each VCI.

The frequency deviation of autonomous sharing controller based primary control is decided by the quadrature output current and the magnitude-frequency characteristics of PR controller closed-loop transfer function in voltage control loop. Thus, the resonant frequency of PR controller is a control

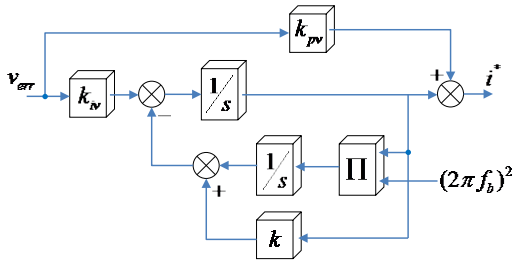

Fig.4. The PR controller with variable resonant frequency.

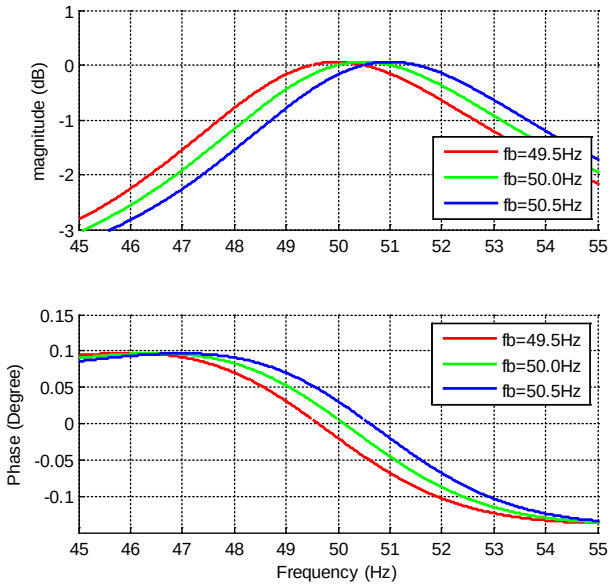

Fig.5. The bode diagram of closed-loop transfer function with different resonant frequency of PR voltage controller.

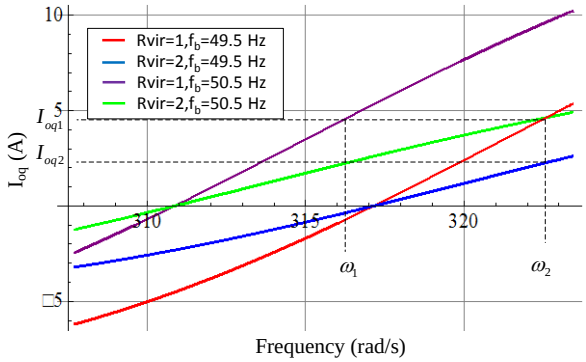

Fig.6. The $I_{oq}-\omega$ droop relationship with different resonant frequency of PR voltage controller.

variable of the primary control level, as shown in Fig. 2. The block diagram of the PR controller with variable resonant frequency is shown in Fig. 4. It can be seen that the ZPD is varied according to the different resonant frequency as shown in Fig. 5. Therefore, the frequency of VCI with the proposed primary control can be changed by tuning the resonant frequency of PR voltage controller.

The $I_{oq}-\omega$ droop relationship with different resonant frequency of PR voltage controller is shown in Fig. 6. It can be seen that the curves are moved when the resonant frequency (f_b) of PR voltage controller is shifted without affecting the *q*-axis output current sharing ratio.

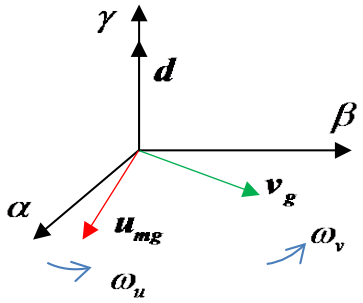

Fig. 7 The control principle of synchronization loop.

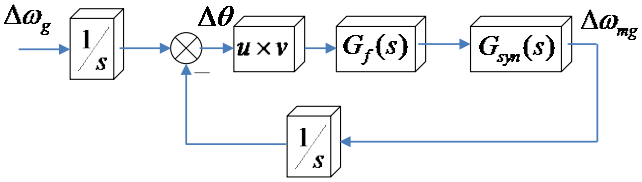

Fig.8. Linearized model of frequency/phase synchronization loop.

B. *Secondary control level*

Secondary control includes frequency and magnitude restoration control loop and synchronization control loop. It can compensate frequency and voltage magnitude deviations to improve the power quality especially in standalone mode and to synchronize the voltages between the VCIs and between to the PCC before connecting one VCI to other VCIs or the main grid.

Two PI control loops are used to restore the frequency and amplitude deviations as shown below:

$$\begin{cases} \Delta\omega_{rest} = k_{p\omega\_rest}(\omega^* - \omega_{mg}) + k_{i\omega\_rest}\int(\omega^* - \omega_{mg})dt \\ \Delta V_{rest} = k_{pE\_rest}(V^* - V_{mg}) + k_{iE\_rest}\int(V^* - V_{mg})dt \end{cases} \quad (8)$$

where $k_{p\omega\_rest}$, $k_{i\omega\_rest}$, k_{pE_rest}, and k_{iE_rest} are the parameters of frequency and amplitude restoration PI controllers.

Phase synchronization process is implemented by using the $\alpha\beta$ components of the PCC voltage ($\boldsymbol{v}_{mg}$) and the VCI output voltage ($\boldsymbol{v}_{VCI}$). If both voltages are synchronized, the cross product should equal to zero [18], as shown in Fig. 7 and the following relationship:

$$\boldsymbol{v}_{VCI\alpha\beta} \times \boldsymbol{v}_{mg\alpha\beta} = 0 \quad \Rightarrow \quad -v_{VCI\alpha}v_{mg\beta} + v_{VCI\beta}v_{mg\alpha} = 0 \quad (9)$$

The linear model for synchronization is shown in Fig. 8, in which a low pass filter $G_f(s)$ is adopted for filter the high frequency component resulting from vector multiplication, while a PI controller $G_{syn}(s)$ is used to guarantee the zero steady state error for frequency/phase synchronization.

Meanwhile, another PI controller is employed to handle the voltage magnitude synchronization.

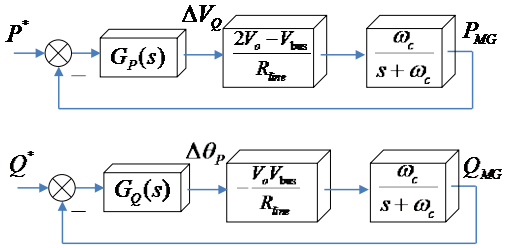

Fig.9. The active and reactive controller in tertiary control

C. *Tertiary control level*

The tertiary control regulates the power flows between the utility grid and MG at PCC.

The above primary and secondary control levels can guarantee the standalone operation of the MG and fulfil the power quality requirements. A tertiary control is necessary to ensure to inject the dispatched power to the main grid. In tertiary level, two PI controllers are used for active and reactive power separately to control the output power of the MG following the power references, as shown in Fig. 9. Note that, in primary control, the novel controller endows to the system fast response speed and control precision in contrast to the conventional droop control as it does not require calculating any active or reactive power. In tertiary control level, the power calculation can be used without effecting dynamic performance the current sharing in primary control due to the inherent low bandwidth characteristic of tertiary control. The outputs of tertiary control can be derived as follows:

$$\begin{aligned}\Delta V_P &= k_{pP}(P^* - P_{MG}) + k_{iP}\int (P^* - P_{MG})dt \\ \Delta\theta_Q &= k_{pQ}(Q^* - Q_{MG}) + k_{iQ}\int (Q^* - Q_{MG})dt\end{aligned} \tag{10}$$

where K_{pP} and K_{iP} are the proportional and integral terms of the PI controller for active power. K_{pQ} and K_{iQ} the proportional and integral terms of the PI controller for reactive power. P^* and Q^* are the reference values of the active and reactive power which need to be injected to the main grid. P_{MG} and Q_{MG} are the output power of MG.

As the output signals of secondary control and tertiary control are sent back to the primary control of each DG unit, the modified voltage reference magnitude/phase, and resonant frequency of PR voltage controller can be expressed as follows:

$$\begin{aligned}V_{ref} &= V_{base} + \Delta V_{syn}^{inv} + \Delta V_{syn}^{grid} + \Delta V_{rest} + \Delta V_P \\ \theta_{ref} &= \theta_{PLL} + \Delta\theta_Q \\ \omega_{ref} &= \omega_{base} + \Delta\omega_{syn}^{inv} + \Delta\omega_{syn}^{grid} + \Delta\omega_{rest}\end{aligned} \tag{11}$$

Where V_{base} and ω_{base} is the fundamental voltage magnitude and angular frequency, ΔV_{syn}^{inv}, $\Delta\omega_{syn}^{inv}$, $\Delta\omega_{syn}^{grid}$ and ΔV_{syn}^{grid} are the synchronization signals of magnitude and angular frequency for synchronization control both between the paralleled inverters and the main grid, ΔV_{rest} and $\Delta\omega_{rest}$ are the restoration signal for voltage magnitude and angular frequency deviation, ΔV_P and $\Delta\theta_Q$ are the control signal from tertiary control.

IV. Simulation and Experimental Results

In order to verify the effectiveness of the novel current autonomous sharing controller based hierarchical control system for MG. The simulation model is built based on Fig.2 in Matlab/Simulink. The simulation model is composed of two paralleled VCIs, a common load powered by the grid utility. Each VCI is connected with local sensitive loads. The control parameters of simulation model are shown in the Table I.

With the objective of testing the proposed hierarchical control strategy in all possible working conditions, the simulation is divided into 9 scenarios, as shown in Fig. 10. Fig. 10 (a) shows the output voltage and current of the MG, and the output current of inverter #1. Fig. 10 (b) shows the active and reactive power, direct and quadrature currents, and system frequency of the paralleled VCIs based MG. The details are

TABLE I
Control Parameters of Simulation

	Parameters		Value
		Description	
Electrical Circuit	V_{dc}	DC Voltage	650 V
	V_{MG}	MG Voltage	311 V
	f	Grid Frequency	50 Hz
	L_f	Filter Inductance	1.8 mH
	C_f	Filter Capacitance	9.9 μF
Loads	Z_{load1}	Load of Inverter #1	800 W+400 Var
	Z_{load2}	Load of Inverter #2	400 W+200 Var
	Z_{com}	Common load	200 W + 50 Var
	Z_{dist}	Disturbance load	800 W + 400 Var
Primary	k_{pv}	Voltage proportional term	0.04
	k_{iv}	Voltage resonant term	93.839
	k_{pi}	Current proportional term	0.07
	k_{pPLL}	PLL proportional term	1.4
	k_{iPLL}	PLL integral term	2000
	R_{vir1}	VR of inverter #1	1 Ω
	R_{vir2}	VR of inverter #2	2 Ω
Secondary	$k_{p\omega\_inv}$	Sync. proportional term for ω	5e-5
	$k_{i\omega\_inv}$	Sync. integral term for ω	1e-3
	k_{pE_inv}	Sync. proportional term for E	0.1
	k_{iE_inv}	Sync. integral term for E	1
	$k_{p\omega\_rest}$	Restoration parameter for ω	1
	$k_{i\omega\_rest}$	Restoration parameter for ω	4
	k_{pE_rest}	Restoration parameter for E	1
	$k_{i\_E\_rest}$	Restoration parameter for E	10
	$k_{p\omega\_grid}$	Sync. proportional term for ω	5e-3
	$k_{i\omega\_grid}$	Sync. integral term for ω	5e-5
	k_{pE_grid}	Sync. proportional term for E	10
	k_{iE_grid}	Sync. integral term for E	0.1
Tertiary	k_{pP}	Proportional term for P_{mg}	5e-2
	k_{iP}	Integral term for P_{mg}	5e-1
	k_{pQ}	Proportional term for Q_{mg}	8e-5
	k_{iQ}	Integral term for Q_{mg}	4e-4
	P^*	P reference of Grid-feeding	500 W
	Q^*	Q reference of Grid-feeding	200 var
	$P^*_{disturb}$	P disturbance of Grid-feeding	1000 W
	$Q^*_{disturb}$	Q disturbance of Grid-feeding	400 var

discussed in the following time stages:

- S1 (0s-2s): The two autonomous current sharing controllers based VCIs operate in standalone mode separately with their own local sensitive loads. The output power of each VCI is determined by the local loads.
- S2 (2s-8s): The frequency and amplitude synchronization controller in secondary control of VCI #2 start to work at 2s. VCI #2 adjusts its output voltage according to the frequency and phase as well as amplitude of MG bus voltage. The settling time of synchronization process is around 2.5s, and then VCI #2 is connected to VCI #1 at 8s.
- S3 (8s-10s): The two VCIs operate in parallel to share local loads based on the novel autonomous current sharing controller. As the *dq* virtual impedances of VCIs are equal to each other, the output active and reactive powers of VCIs are same (600 W+j300 var).
- S4 (10s-16s): The frequency and voltage magnitude restoration loops in secondary control start to act at 10s to compensate the frequency and magnitude deviations resulting from the inherent droop characteristics of the primary control. The MG bus frequency is restored to 50 Hz immediately. Therefore, the power quality of supplement is improved in islanded mode.
- S5 (16s-24s): The frequency of MG bus start to fluctuate at 16s because that the grid synchronization loop in secondary control is activated to synchronize the frequency/phase and magnitude of MG bus voltage to the voltage of PCC. The output of synchronization controller is transmitted through communication link. All the VCIs in MG adjust their voltage reference simultaneously. The transient process lasts around 2.5s with the peak of 53 Hz.
- S6 (24s-30s): The MG is connected to the main grid at 24s by turning on the STS for transferring the MG from islanded mode to grid-connected mode. Meanwhile, the active and reactive power flow controllers in tertiary control level are activated. The phase and amplitude increments of MG bus voltage are calculated according to the errors of the power reference (P^* and Q^*) and the injected power. Then, these increments are transmitted to VCIs for controlling MG to inject the required active and reactive powers to the grid utility. As the excellent

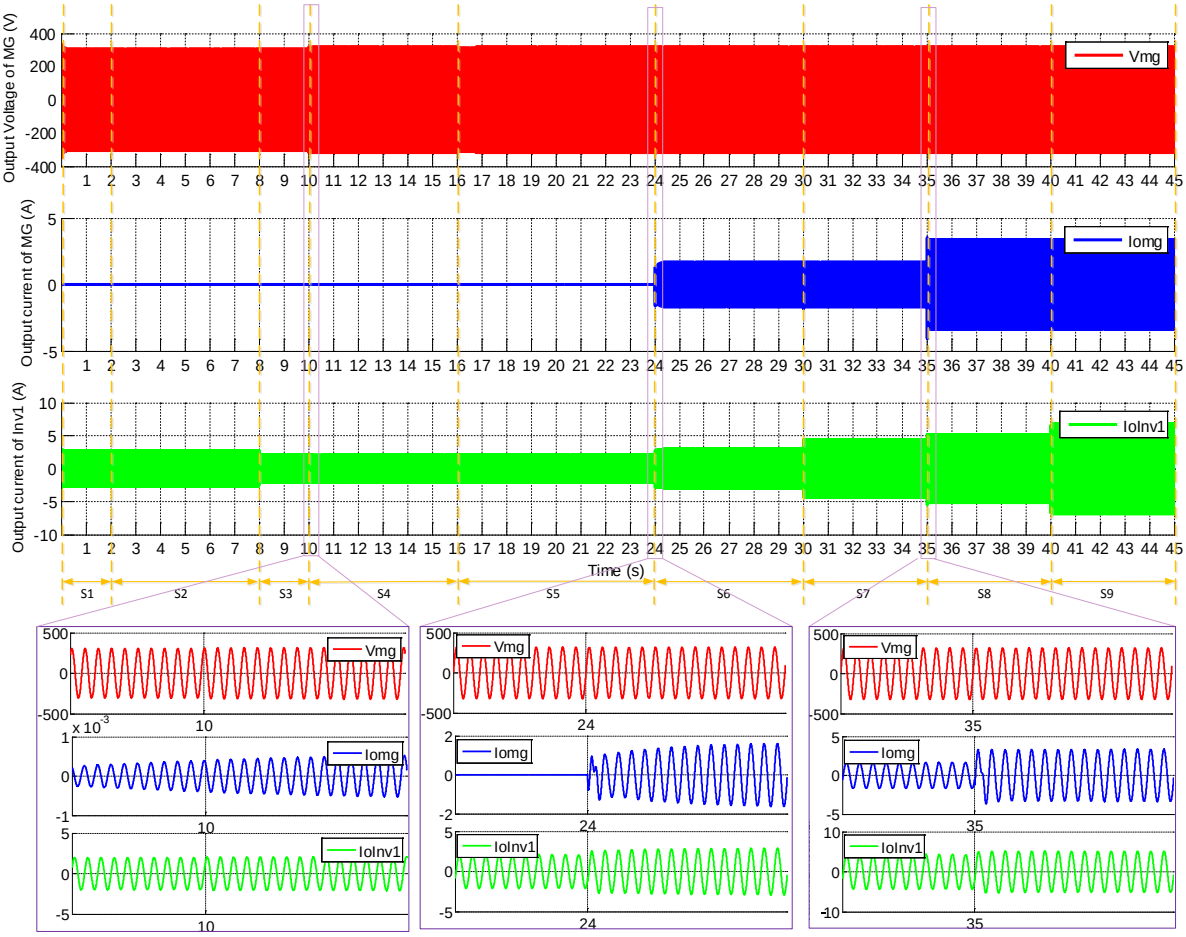

(a)

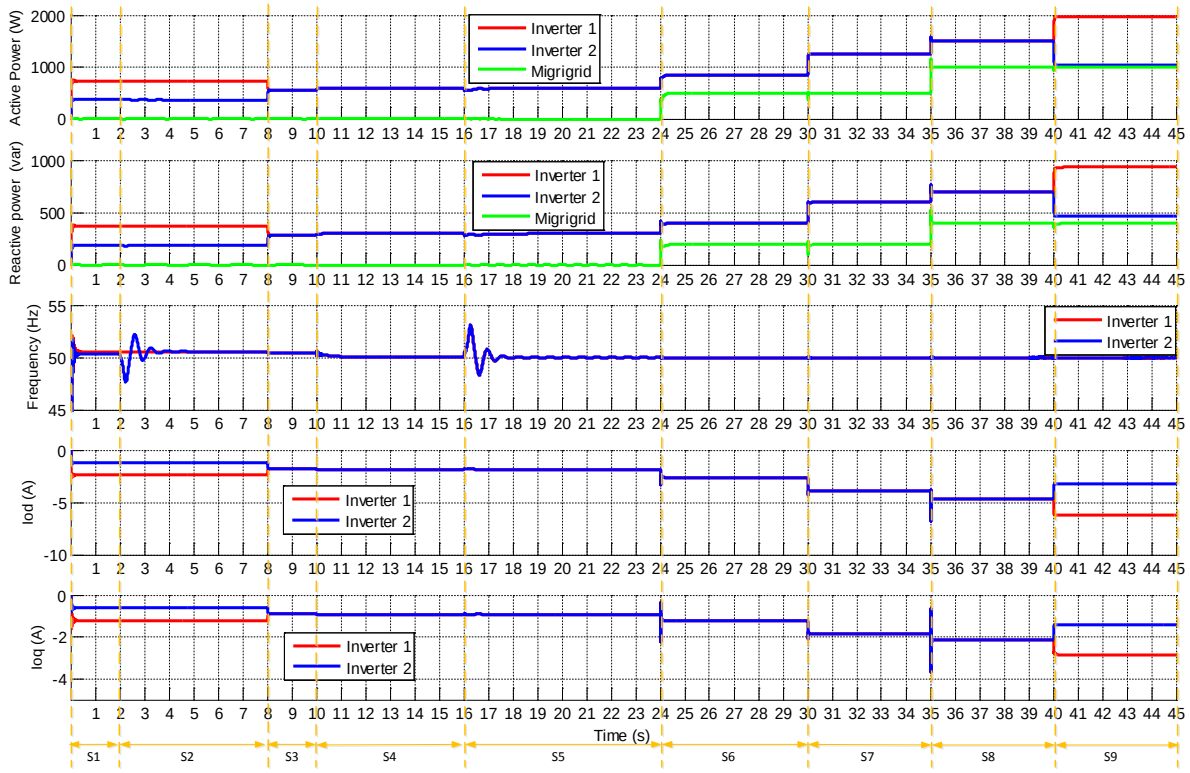

(b)

Fig.10. Simulation results of the hierarchical controlled grid-connected MG

dynamic response of the proposed autonomous current sharing controller in primary control, the dynamic response of grid-feeding power changes is guaranteed.

- S7 (30s-35s): A load step up disturbance (Z_{dist}) in the MG is carried out for testing the performance of proposed hierarchical control. It can be seen that the output power of each VCI is increased immediately to supply the local sensitive load by the primary control. However the power delivered from MG to the main grid is not affected in steady state which is kept constant to follow the power reference by means of the tertiary control. Therefore, the proposed hierarchical control strategy can achieve the decoupled control.

- S8 (35s-40s): A power reference step up disturbance ($P^*_{disturb}$+j$Q^*_{disturb}$) at 35s is carried out to test the dynamic response and dispatched power reference tracking steady state performance of the proposed hierarchical control strategy. The grid-feeding power of the MG is increased rapidly and smoothly according to the power reference, which means the MG with proposed hierarchical control strategy can increase the reliability and availability to the grid utility by provide the required power.

- S9 (40s-45s): The active and reactive power sharing ratio of two VCIs in MG is changed from 1:1 to 1:2 at 40s. As it can be observed, the output active and active powers of VCIs are changed immediately according to the new power sharing ratio. Moreover, the dispatched power of MG to the grid utility maintain to the power reference. This will endow the MG more flexibility for sharing the active and reactive loads.

V. Conclusion

A hierarchical control system based on a novel autonomous current sharing controller for grid-connected MG is presented in this paper. The three-level hierarchical control system is able to guarantee the power sharing performance among voltage controlled parallel inverters, while injecting the required active and reactive power to the utility grid. The primary and secondary control levels can achieve the power sharing performance and power supply quality in standalone operation. The tertiary control level is thereafter employed to perform the connection to the utility grid. Simulation results from a two grid-connected paralleled VCIs system are shown to verify the effectiveness of the designed system.

References

[1] Guerrero, J.M.; Poh Chiang Loh; Tzung-Lin Lee; Chandorkar, M., "Advanced Control Architectures for Intelligent Microgrids—Part II: Power Quality, Energy Storage, and AC/DC Microgrids," *Industrial Electronics, IEEE Transactions on*, vol.60, no.4, pp.1263,1270, April 2013

[2] Lasseter, R.H., "MicroGrids," Power Engineering Society Winter Meeting, 2002. IEEE , vol.1, no., pp.305-308, 2002

[3] M. Dai, M. Marwali, J. Jung, and A. Keyhani, "Power flow control of a single distributed generation unit," *IEEE Trans. Power Electron*., vol. 23, no. 1, pp. 343–352, Jan. 2008.

[4] Yunwei Li, Vilathgamuwa, D.M., Poh Chiang Loh, "Design, Analysis, and Real-Time Testing of a Controller for Multibus Microgrid System," *IEEE Transactions on Power Electronics*, vol. 19, no. 5, pp. 1195–1204, Sept. 2004.

[5] Guerrero, J.M., Garcia De Vicuna, L., Matas, J., Castilla, M., Miret, J., "Output Impedance Design of Parallel-Connected UPS Inverters With Wireless Load-Sharing Control," *IEEE Transactions on Industrial Electronics*, vol. 52, no. 4, 1126-1135, Aug. 2005

[6] J. Guerrero, L. de Vicuna, J. Matas, M. Castilla, and J. Miret, "A wireless controller to enhance dynamic performance of parallel inverters in distributed generation system," *IEEE Trans. Power Electron*., vol. 19, no. 5, pp. 1205–1213, Sep. 2004.

[7] C. Sao and P. Lehn, "Autonomous load sharing of voltage source converters," *IEEE Trans. Power Del*., vol. 20, no. 2, pp. 1009–1016, Apr. 2005.

[8] Guerrero, J.M., Matas, J., Luis Garcia de Vicuna, Castilla, M., Miret, J., "Decentralized Control for Parallel Operation of Distributed Generation Inverters Using Resistive Output Impedance," *Industrial Electronics, IEEE Transactions on*, vol.54, no.2, pp.994,-1004, April Apr. 2007

[9] Y. W. Li and C. N. Kao, "An accurate power control strategy for power electronics- interfaced distributed generation units operating in a low voltage multibus microgrid," *IEEE Trans. Power Electron*, vol. 24, no. 12, pp. 2977–2988, Dec. 2009.

[10] Engler A，Soultanis N．"Droop control in LV-grids[C]"// *International Conference on Future Power Systems*，USA：IEEE，2005：1-6.

[11] Guerrero, J.M.; Matas, J.; Luis Garcia de Vicuna; Castilla, M.; Miret, J., "Decentralized Control for Parallel Operation of Distributed Generation Inverters Using Resistive Output Impedance," Industrial Electronics, IEEE Transactions on , vol.54, no.2, pp.994,-1004, April Apr. 2007

[12] Yasser Abdel-Rady Ibrahim Mohamed, Ehab F. El-Saadany. "Adaptive Decentralized Droop Controller to Preserve Power Sharing Stability of Paralleled Inverters in Distributed Generation Microgrids," *IEEE Transactions on Power Electronics*, vol. 23, no. 6, pp.2806-2816, Nov. 2008

[13] Guerrero, J.M.; Chandorkar, M.; Lee, T.; Loh, P.C., "Advanced Control Architectures for Intelligent Microgrids—Part I: Decentralized and Hierarchical Control," *Industrial Electronics, IEEE Transactions on*, vol.60, no.4, pp.1254-1262, April 2013.

[14] A. Bidram and A. Davoudi, "Hierarchical structure of microgrids control systems," *IEEE Trans. Smart Grid*, vol. 3, no. 4, pp. 1963–1976, 2012

[15] Xiaonan Lu, Guerrero, J.M., Kai Sun, Vasquez, J.C., Teodorescu, R., Lipei Huang, "Hierarchical Control of Parallel AC-DC Converter Interfaces for Hybrid Microgrids," *Smart Grid, IEEE Transactions on*, vol.5, no.2, pp.683-692, March. 2014.

[16] Guerrero, J.M., Vasquez, J.C., Matas, J., de Vicuña, L.G., Castilla, M., "Hierarchical Control of Droop-Controlled AC and DC Microgrids—A General Approach Toward Standardization," *Industrial Electronics, IEEE Transactions on*, vol. 58, no. 1, pp. 158 - 172, Jan. 2011.

[17] Shafiee, Q., Vasquez, J.C., Guerrero, J.M., "Distributed Secondary Control for Islanded Microgrids—A Novel Approach," *Power Electronics, IEEE Transactions on*, vol. 29, no. 2, pp. 1018 - 1031, Feb. 2014.

[18] Vasquez, J.C., Guerrero, J.M., Savaghebi, M., Eloy-Garcia, J., Teodorescu, R., "Modeling, Analysis, and Design of Stationary-Reference-Frame Droop-Controlled Parallel Three-Phase Voltage Source Inverters," *Industrial Electronics, IEEE Transactions on*, vol. 60, no. 4, pp. 1271–1280, April 2013.